Published in final edited form as:
Ophthalmology. 2014 March ; 121(3): 719–726. doi:10.1016/j.ophtha.2013.10.014.

EN FACE ENHANCED-DEPTH SWEPT-SOURCE OPTICAL COHERENCE TOMOGRAPHY FEATURES OF CHRONIC CENTRAL SEROUS CHORIORETINOPATHY

Daniela Ferrara, MD PhD[1], **Kathrin J. Mohler, BS**[2,3], **Nadia Waheed, MD MPH**[1], **Mehreen Adhi, MBBS**[1], **Jonathan J. Liu, MS**[2], **Ireneusz Grulkowski, PhD**[2], **Martin F. Kraus, Dipl.**[2,4], **Caroline Baumal, MD**[1], **Joachim Hornegger, PhD**[4], **James G. Fujimoto, PhD**[2], and **Jay S. Duker, MD**[1]

[1]New England Eye Center, Tufts Medical Center, Boston, Massachusetts, USA

[2]Department of Electrical Engineering and Computer Science and Research Laboratory of Electronics, Massachusetts Institute of Technology, Cambridge, Massachusetts, USA

[3]Faculty of Physics, Ludwig-Maximilians-University Munich, Munich, Germany

[4]Pattern Recognition Lab and Graduate School in Advanced Optical Technologies, University Erlangen-Nuremburg, Erlangen-Nuremburg, Germany

Abstract

Purpose—To characterize en face features of the retinal pigment epithelium (RPE) and choroid in eyes with chronic central serous chorioretinopathy (CSCR) using a high-speed, enhanced-depth swept-source optical coherence tomography (SS-OCT) prototype.

Design—Consecutive patients with chronic CSCR were prospectively examined with SS-OCT.

Participants—Fifteen eyes of 13 patients.

Methods—Three-dimensional 6×6mm macular cube raster scans were obtained with SS-OCT operating at 1050nm wavelength and 100,000 A-lines/sec with 6μm axial resolution. Segmentation of the RPE generated a reference surface; en face SS-OCT images of the RPE and choroid were extracted at varying depths every 3.5 μm (1 pixel). Abnormal features were characterized by systematic analysis of multimodal fundus imaging including color photographs, fundus autofluorescence, and fluorescein and indocyanine-green angiography (ICGA).

Main Outcome Measures—En face SS-OCT morphology of the RPE and individual choroidal layers.

Results—In all eyes, 15/15 (100%) en face SS-OCT imaging at the RPE level revealed absence of signal corresponding to RPE detachment and/or RPE loss. En face SS-OCT imaging at the choriocapillaris level showed focally enlarged vessels in 8 of 15 eyes (53%). At the level of

Corresponding Author: Jay S. Duker, Mailing address: 800 Washington Street, Box 450, Boston, MA 02111, Phone: +1 (617) 636-4677 / Fax: +1 (617) 636-4215, jduker@tuftsmedicalcenter.org.

Conflict of Interest: *Martin Kraus* has a patent owned by MIT and licensed to Optovue, Inc. *James G. Fujimoto* has personal financial interest on Optovue, Inc. and patents owned by MIT and licensed to Carl Zeiss Meditech, Inc. and Optovue, Inc. *Jay S. Duker* receives research support from Carl Zeiss Meditech, Inc. and Optovue, Inc.

Sattler's layer, en face SS-OCT documented focal choroidal dilation in 8 of 15 eyes (53%) and diffuse choroidal dilation in 7 of 15 eyes (47%). At the level of Haller's layer, these same features were observed in 3 of 15 eyes (20%) and 12 of 15 eyes (80%) respectively. In all affected eyes, these choroidal vascular abnormalities were seen just below areas of RPE abnormalities. In 2 eyes with secondary choroidal neovascularization, distinct en face SS-OCT features corresponded to the neovascular lesions.

Conclusions—High-speed, enhanced-depth SS-OCT at 1050 nm wavelength enables the visualization of pathological features of the RPE and choroid in eyes with chronic CSCR not usually appreciated with standard spectral domain (SD) OCT. En face SS-OCT imaging appears to be a useful tool in the identification of choroidal neovascularization without the use of angiography. This *in vivo* documentation of the RPE and choroidal vasculature at variable depths may help elucidate the pathophysiology of disease and can potentially contribute to the diagnosis and management of chronic CSCR.

Central serous chorioretinopathy (CSCR) is characterized by one or more serous detachments of the neurosensory retina commonly associated with retinal pigment epithelium (RPE) detachments. There is a broad spectrum of clinical presentations.[1-6] CSCR tends to affect the retina primarily in the macular area, but multifocal or extensive retinal involvement can also occur, as well as inferior serous retinal detachment.[3,7] Symptoms are self-limited in most of the cases, but the disease can be recurrent or bilateral in approximately one third.[8,9] Although the visual prognosis is usually good in acute manifestations, RPE loss, geographic atrophy, chronic cystic retinal changes, subretinal fibrinous accumulation, subretinal fibrosis and/or secondary choroidal neovascularization (CNV) are known late complications that can be associated with permanent visual loss.[10] Clinical and epidemiological evidence points to a relationship between CSCR and elevated levels of circulating catecholamines and corticosteroids, from either exogenous or endogenous sources. Interestingly, local injections of corticosteroids do not seem to induce the disease often.[3,11-21] The pathophysiology of this intriguing condition remains unknown. Functional and morphological features on indocyanine-green angiography (ICGA) and optical coherence tomography (OCT) strongly suggest that the choroid is primarily involved. Choroidal hyperpermeability, vascular congestion, and increased choroidal thickness were found to be hallmarks of the entity.[22,23]

Three-dimensional OCT is a useful tool in the investigation of chorioretinal disorders.[24,25] However, the detailed assessment of the choroid is fundamentally limited in commercially available spectral/Fourier domain (SD)-OCT devices, even when applying the enhanced depth imaging strategy for imaging acquisition.[22,26] Swept-source (SS)-OCT is a Fourier domain depth-resolved method that uses a wavelength-tunable laser and a dual-balanced photo detector instead of a broadband super-luminescent diode, spectrometer and high-speed line-scan camera that are used in SD-OCT. SS-OCT technology offers several potential advantages in comparison to SD-OCT, including higher imaging speeds, higher detection efficiencies, improved imaging range, reduced sensitivity roll off with imaging depth, and adaptability to longer imaging wavelengths.[27,28] This study characterized three-dimensional en face features of the RPE and choroid in eyes with chronic CSCR using a novel, high-speed, high-resolution, enhanced-depth SS-OCT prototype with improved tissue penetration at 1050 nm wavelength.

METHODS

This study was performed under approved institutional review board protocols from the New England Eye Center and Massachusetts Institute of Technology. The research adhered to the tenets of the Declaration of Helsinki and complied with the Health Insurance Portability and Accountability Act of 1996. Signed informed consent was obtained before

SS-OCT examination. Consecutive patients examined at the New England Eye Center between October 2012 and April 2013 with the clinical diagnosis of chronic CSCR as defined by idiopathic, single or multiple serous detachments of the neurosensory retina in the macular area associated with RPE changes or RPE leaks on fluorescein angiography and visual symptoms for at least 6 months were offered enrollment in the study in a prospective fashion. Exclusion criteria were any associated, previous or concomitant ophthalmological condition that could confound the interpretation of multimodal fundus imaging, or history of previous treatment for CSCR including thermal laser photocoagulation, photodynamic therapy or intravitreal administration of anti-vascular endothelial growth factor.

Enrolled patients received a complete ophthalmological examination including assessment of best corrected visual acuity (BCVA), biomicroscopy, intra-ocular pressure, and a dilated fundus examination. Patients were examined with a SS-OCT prototype system operating at 1050 nm for enhanced choroidal penetration, similar to that described by Potsaid et al.[27,29] The system employs a commercially available 100 kHz wavelength-swept semiconductor laser (Axsun Technologies Inc.) with a sweep bandwidth of ~100 nm providing an axial resolution of 6 μm in tissue. The light incident on the eye was 1.9 mW which is consistent with the American National Standard Institute (ANSI) standards for safe ocular exposure.[30] Three-dimensional 6×6mm macular cube raster scans with 400×400 axial scans were obtained, each acquired within 1.7 seconds. For each patient, at least two volumetric scans with orthogonal fast scan directions were acquired, processed with software for motion correction and merged into a single volumetric dataset to increase the signal.[31] An intensity and gradient based, semi-automatic algorithm was used to segment the RPE or Bruch's membrane in regions of RPE detachment in order to generate a reference surface for en face display.[32] En face images of the RPE and choroid were extracted at varying depths every 3.5 μm (1pixel, corresponding to the digital resolution of OCT images) from the RPE / Bruch's membrane reference surface. This analysis permitted point-to-point correlation between en face images and cross-sectional b-scan images. Atypical features appearing on the en face images were characterized by systematic analysis of multimodal fundus imaging records including color fundus picture, fundus autofluorescence, fluorescein angiography (FA) and indocyanine-green angiography (ICGA).

RESULTS

Fifteen eyes of 13 patients seen consecutively and diagnosed with chronic CSCR were enrolled in the study. Their baseline characteristics were as follows: 11 males, 10 Caucasian and 3 Asian, mean age 50.7 years (SD ± 9.5 years) and mean BCVA 20/50 (range 20/20 to 20/800). All enrolled patients had a history of at least 6 months of visual symptoms in the affected eye(s). The mean period of time since initial presentation was 13.6 months (range 6 to 60 months). The mean choroidal thickness assessed on SS-OCT b-scans at the center of the fovea was found to be 351 μm (SD ± 84 μm), which is thicker than the mean choroidal thickness determined by SD-OCT previously reported for normal subjects in this age group (287 μm; SD ± 76 μm).[33] En face SS-OCT images, or c-scans, were obtained from the three-dimensional SS-OCT data sets. The en face imaging allowed virtual sectioning of the macular area in consecutive c-scans 3.5 μm apart from each other, from the vitreous cavity to the sclera. Representative c-scans of the RPE layer, choriocapillaris, and choroidal layers with medium size vessels (inner choroid or the so-called Sattler's layer) and large size vessels (outer choroid or the so-called Haller's layer) were obtained. C-scans above the RPE layer, in order to completely characterize the en face SS-OCT features of retinal pigment epithelium detachments (PED) were also generated.

En face SS-OCT images at the RPE level revealed specific changes in all eyes, which correlated with pathological changes seen on cross-sectional SS-OCT and multimodal

imaging including fundus autofluorescence, FA and ICGA. Absence of SS-OCT signal at the RPE level corresponded to RPE detachment or loss (Figure 1) and was observed in all eyes. One eye with RPE leakage at the center of the macula characterized by the classic “ink blot” appearance on FA had the exact corresponding point of RPE disruption visible on en face SS-OCT (Figure 2). Of note, en face OCT images extracted from slightly above the RPE level showed large hypo-echoic areas of absent signal corresponding to fluid accumulation associated with either neurosensory retinal detachment or RPE detachment. Neurosensory detachments present with smooth borders between the fluid and the dome-shaped retina; while RPE detachments show a characteristic, distinct hyper-echoic halo corresponding to the dome-shaped RPE (Figure 2). Within the area of neurosensory retinal detachment, heterogeneous SS-OCT signal with numerous optically dense dots was observed in some cases, corresponding to photoreceptors and RPE debris seen on b-scans (Figure 3, available at http://aaojournal.org).

En face SS-OCT imaging at the level of the choriocapillaris showed hypo-echoic spots suggesting the presence of enlarged vessels at this level in 8 eyes (53%), but images were unremarkable in the other 7 eyes. It was unclear whether the absence of identifiable choriocapillary changes in the unremarkable eyes (47%) was related to a limitation in image resolution, given the smaller vascular lumen and the complexity vascular anatomy at this level, or the true absence of vascular engorgement. In all affected eyes, the choriocapillaris changes were grossly underlying RPE changes, either PED or RPE loss (Figure 2) seen on b-scans and further documented on fundus autofluorescence and FA. These choriocapillary changes corresponded to hyper-fluorescent spots on ICGA.

Choroidal en face SS-OCT imaging at the level of Sattler’s layer revealed dilation of medium size choroidal vessels in two somewhat distinct patterns. In 7 eyes (47%), relatively homogeneous dilation of vessels was observed in the entire series of en face images from this layer, which was characterized as “diffuse choroidal dilation” (Figure 3-I, available at http://aaojournal.org). In 8 eyes (53%), some vascular branches were found to have much bigger calibers than the surrounding enlarged choroidal vessels and were characterized as “focal choroidal dilation” (Figure 4-I, available at http://aaojournal.org). Similarly, SS-OCT en face images representative of Haller’s layer revealed diffuse choroidal dilation in 12 eyes (80%)(Figure1-F), and focal choroidal dilation in 3 eyes (20%). Comparison of different image modalities revealed a correspondence between focal and diffuse choroidal dilation on en face OCT images and hyperfluorescent areas on ICGA typically described as choroidal hyperperfusion (Figure 4-H and I, available at http://aaojournal.org). No correlation could be established between choroidal changes and patients’ age or gender, or the duration of symptoms.

En face SS-OCT images revealed CNV in 2 eyes, corresponding to the diagnosis of CNV initially determined by clinical exam, FA and ICGA. In one case, comparison of different image modalities showed subretinal fibrosis in the center of the macula with only residual exudation from choroidal neovascularization and shallow subretinal fluid accumulation. Middle to late phase ICGA showed one polypoidal-like formation on the topography of the fibrosis. En face SS-OCT imaging at the level of the Bruch’s membrane clearly delineated an abnormal appearing neovascular network underlying the fibrosis, one of whose branches was terminating in the topography of the polypoidal-like lesion seen on ICGA. En face SS-OCT imaging at the level of the choriocapillaris showed a distinct, round area with hyporeflective signal, connecting to the center of the neovascular network. SS-OCT en face images from the medium and large choroidal vessel layers showed diffuse choroidal dilation (Figure 5). In the other case with secondary CNV comparison of different imaging modalities showed a subretinal lesion in the center of the macula, limited exudation on FA, and hyperfluorescent spot in the middle to late phase ICGA. In this eye, en face SS-OCT

imaging throughout the choroid revealed a distinct, round area with hyporeflective signal underneath the subretinal lesion. This area seemed to be connected to the CNV through a defect in the RPE, and connected to a large choroidal vessel in the en face images from deeper levels. These features were also observed in cross-sectional SS-OCT images through the fovea (Figure 6).

DISCUSSION

Serous detachment of the neurosensory retina is characteristic of the typical presentation of CSCR, but the source of the subretinal fluid is still not completely agreed upon.[1,9] Retinal pigment epithelium detachments have been identified in up to 63% of affected eyes when studied with angiography and cross-sectional OCT imaging, and may or may not be associated with neurosensory retinal detachments or clinical symptoms.[9] Since fluorescein angiography shows focal, single or multiple leaks from the RPE that are characteristic of the entity, focal or diffuse RPE dysfunction has been previously hypothesized as the primary pathological mechanism in CSCR.[34,35] However, additional morphological features derived from old and new investigative results challenge this hypothesis. Retinal changes may represent a later stage in disease evolution, while the choroid seems to be primarily affected.[22,23] In our group of patients with chronic CSCR, en face SS-OCT images documented PEDs in all eyes, as well as morphological changes in the choroid underneath and beyond RPE changes.

It has been proposed that ischemia or impaired autoregulation of choroidal circulation – potentially related to hypercortisolism, systemic hypertension, and sympathetic deregulation – may play a role in choroidal hyperpermeability on CSCR.[9,36-40] Congested and dilated choroidal capillaries and veins, choroidal staining, and leakage into the interstitial space are commonly seen on ICGA. These widespread areas of abnormal choroidal circulation can occur throughout the posterior pole, even from sites not seen on fluorescein angiography.[38,41] Abnormalities in one or more lobules can be frequently observed in both symptomatic and asymptomatic eyes, as well as in unaffected fellow eyes.[23,36] Nonetheless, ICGA does not show hyperfluorescence in all cases of chronic CSCR.[42] Previous studies reported increased choroidal thickness observed on cross-sectional OCT images with no corresponding changes on ICGA.[23] This incidental inconsistency between the two imaging methods might indicate a relative limitation of ICGA in identifying particular alterations of the choroidal morphology in CSCR. The interpretation of the angiogram is affected by numerous factors, related to some extent to the nature of the examination and to techniques of image acquisition. Moreover, the two dimensional nature of the ICGA means that all choroidal layers overlap in the angiogram, which makes it difficult to identify the individual layers (Figure 3, available at http://aaojournal.org). Based on the visualization of three-dimensional SS-OCT data, we were able to characterize individual layers of the retina and choroid. On the other hand, the focal and diffuse choroidal dilations we observed on en face SS-OCT images did correspond to hyperfluorescent areas on ICGA (Figure 2 and Figure 4, available at http://aaojournal.org). Of note, these particular morphological changes of the choroidal vasculature that we saw in en face SS-OCT cannot be seen on cross-sectional OCT images. Therefore, en face imaging is superior to cross-sectional imaging for visualizing these features.

The natural course of the disease and the occurrence of secondary complications are highly variable and somewhat unpredictable in CSCR. The therapeutic response to potentially beneficial interventions ultimately targets choroidal congestion and hyperpermeability.[42,43] Using en face SS-OCT images we observed focal and diffuse vascular dilation at the level of the choriocapillaris in half (53%) of the enrolled eyes, and at the level of Sattler's and Haller's layers in all eyes. In the two eyes with secondary CNV a single, well delineated

area of hypo-echoic SS-OCT signal was observed at the site of the CNV. In the eye with fibrotic CNV, this feature was present at the level of the Bruch's membrane (Figure 5), whereas in the eye with active CNV it was present throughout the choroidal depth, from Bruch's membrane to the choroidal-scleral interface (Figure 6). No definitive conclusions can be made from these two anecdotal cases. Nonetheless, multimodal imaging analysis and three-dimensional OCT visualization of the macular area suggest that our observation might be related to pronounced choroidal vascular dilation or remodeling, or to extracellular fluid accumulation. It also raises the question of whether a better understanding of en face choroidal features could potentially contribute to the differential diagnosis between CSCR and polypoidal choroidal vasculopathy masquerading as CSCR, could potentially indicate eyes of higher risk in developing secondary CNV, or indicate other predictive markers about disease evolution.

En face imaging is complementary to cross sectional imaging and enables visualization of structures which cannot be easily appreciated in cross sectional images. In our group of patients, en face imaging revealed morphological changes in the choroidal vasculature that could not be initially identified on cross sectional images alone; in part because en face imaging documents the vascular anatomy with an orientation comparable to other imaging modalities such as ICGA. Thus, the topographical analysis allowed by en face imaging facilitates the comparison between multiple imaging modalities and permits a better characterization of the morphology and extend of choroidal changes. The topographical documentation on en face OCT also permits a detailed assessment of each individual choroidal layer, which cannot be performed on cross-sectional OCT. This advantage is especially useful in the investigation of the choriocapillaris, due to the reduced thickness of its complex vascular network. However, the en face imaging modality requires high speed acquisition, since each pixel in the en face image requires an axial scan. In this sense, the higher imaging speeds allowed by SS-OCT technology is a fundamental advantage in comparison to SD-OCT. Higher detection efficiencies, improved imaging range, reduced sensitivity roll off with imaging depth, and adaptability to longer imaging wavelengths are other potential advantages of SS-OCT in comparison to SD-OCT, which contributed to the improved image quality of the choroid we achieved using SS-OCT and facilitated the clinical interpretation of the results. To our knowledge, this is the first time distinct choroidal changes are described in eyes with chronic CSCR based on en face SS-OCT. Although the physiopathological significance of focal versus diffuse choroidal dilation is still to be determined, our original results may lead to new insights related to disease mechanisms. En face SS-OCT also offers a new approach in the assessment of CNV, and might offer an alternative non-invasive investigative tool in the diagnosis and management of CNV. This test may be useful to understand alterations in the layers underneath the neurosensory retina in pathologies other than CSCR, without requiring venous injection for angiography.

The small number of enrolled patients is a limitation of this study, although strict inclusion and exclusion criteria were applied to assure the reproducibility of the results. These strict criteria are a two-edged sword and could limit generalizability. Future studies with a larger number of patients are needed to establish the frequency of our observations, in both chronic and acute presentations of CSCR as well as in asymptomatic fellow eyes. The use of a new SS-OCT prototype instrument or image processing methods might introduce unexpected imaging artifacts that must be taken into consideration in the interpretation of tomographic findings. The same concern applies to the interpretation of a post-acquisition reconstruction of SS-OCT en face images using a segmentation algorithm. The most significant limitation of en face OCT imaging is that pathologies such as edema or atrophy which cause displacement of retinal or choroidal structure outside of their normal anatomical positions can cause these features to be visualized at different levels of the en face images. En face

images are extracted from the three dimensional OCT data set using a surface referenced to the RPE / Bruch's membrane position, rather than by specifically identifying and segmenting individual layers. Therefore, care must be used in en face image interpretation. In order to support our interpretation of en face SS-OCT images we used point-to-point correlation with cross-sectional SS-OCT b-scans and systematic comparison with other fundus imaging modalities including color fundus photography, fundus autofluorescence, FA and ICGA.

In summary, the high-speed, high-resolution, enhanced-depth SS-OCT prototype operating at 1050 nm wavelength used in this study allowed the characterization of three-dimensional en face features of the RPE and choroid in eyes with chronic CSCR in a fast, secure, non-invasive and reproducible assessment. This new investigative tool revealed morphological features implicated in underlying physiopathological mechanisms, and may in the future potentially contribute to the diagnosis and management of this complex disorder.

Supplementary Material

Refer to Web version on PubMed Central for supplementary material.

Acknowledgments

Financial Support: We acknowledge support from NIH (R01-EY011289-27, R01-EY013178-12, R01-EY018184-05, R44EY022864-01, R01-CA075289-16, R01-NS057476-05, R44-EY022864-01); AFOSR (FA9550-10-1-0551 and FA9550-10-1-0063); Research to Prevent Blindness; Massachusetts Lions Club; German Science Foundation DFG (DFG-GSC80-SAOT). The funding organizations had no role in the design or conduct of this research.

REFERENCES

1. Gass JD. Pathogenesis of disciform detachment of the neuroepithelium. Am J Ophthalmol. 1967; 63(suppl):1–139. [PubMed: 6019308]
2. Yannuzzi LA. Type A behavior and central serous chorioretinopathy. Trans Am Ophthalmol Soc. 1986; 84:799–845. [PubMed: 3590481]
3. Yannuzzi LA, Shakin JL, Fisher YL, Altomonte MA. Peripheral retinal detachments and retinal pigment epithelial atrophic tracts secondary to central serous pigment epitheliopathy. Ophthalmology. 1984; 91:1554–72. [PubMed: 6084221]
4. Spaide RF, Campeas L, Haas A, et al. Central serous chorioretinopathy in younger adults. Ophthalmology. 1996; 103:2070–9. [PubMed: 9003341]
5. Kitzmann AS, Pulido JS, Diehl NN, et al. The incidence of central serous chorioretinopathy in Olmsted County, Minnesota, 1980-2002. Ophthalmology. 2008; 115:169–73. [PubMed: 18166410]
6. Ross A, Ross AH, Mohamed Q. Review and update of central serous chorioretinopathy. Curr Opin Ophthalmol. 2011; 22:166–73. [PubMed: 21427570]
7. Piccolino FC, de la Longrais RR, Ravera G, et al. The foveal photoreceptor layer and visual acuity loss in central serous chorioretinopathy. Am J Ophthalmol. 2005; 139:87–99. [PubMed: 15652832]
8. Gilbert CM, Owens SL, Smith PD, Fine SL. Long-term follow-up of central serous chorioretinopathy. Br J Ophthalmol. 1984; 68:815–20. [PubMed: 6541945]
9. Liew G, Quin G, Gillies M, Fraser-Bell S. Central serous chorioretinopathy: a review of epidemiology and pathophysiology. Clin Experiment Ophthalmol. 2013; 41:201–14. [PubMed: 22788735]
10. Gomolin JE. Choroidal neovascularization and central serous chorioretinopathy. Can J Ophthalmol. 1989; 24:20–3. [PubMed: 2469527]
11. Bouzas EA, Scott MH, Mastorakos G, et al. Central serous chorioretinopathy in endogenous hypercortisolism. Arch Ophthalmol. 1993; 111:1229–33. [PubMed: 8363466]

12. Bouzas EA, Karadimas P, Pournaras CJ. Central serous chorioretinopathy and glucocorticoids. Surv Ophthalmol. 2002; 47:431–48. [PubMed: 12431693]
13. Quillen DA, Gass DM, Brod RD, et al. Central serous chorioretinopathy in women. Ophthalmology. 1996; 103:72–9. [PubMed: 8628563]
14. Carvalho-Recchia CA, Yannuzzi LA, Negrao S, et al. Corticosteroids and central serous chorioretinopathy. Ophthalmology. 2002; 109:1834–7. [PubMed: 12359603]
15. Haimovici R, Rumelt S, Melby J. Endocrine abnormalities in patients with central serous chorioretinopathy. Ophthalmology. 2003; 110:698–703. [PubMed: 12689888]
16. Harada T, Harada K. Six cases of central serous chorioretinopathy induced by systemic corticosteroid therapy. Doc Ophthalmol. 1985; 60:37–44. [PubMed: 4042815]
17. Tittl M, Maar N, Polska E, et al. Choroidal hemodynamic changes during isometric exercise in patients with inactive central serous chorioretinopathy. Invest Ophthalmol Vis Sci. 2005; 46:4717–21. [PubMed: 16303970]
18. Fawzi AA, Holland GN, Kreiger AE, et al. Central serous chorioretinopathy after solid organ transplantation. Ophthalmology. 2006; 113:805–13. [PubMed: 16650676]
19. Thoelen AM, Bernasconi PP, Schmid C, Messmer EP. Central serous chorioretinopathy associated with a carcinoma of the adrenal cortex. Retina. 2000; 20:98–9. [PubMed: 10696758]
20. Fawzi AA, Cunningham ET Jr. Central serous chorioretinopathy after bone marrow transplantation. Am J Ophthalmol. 2001; 131:804–5. [PubMed: 11384585]
21. Rahbani-Nobar MB, Javadzadeh A, Ghojazadeh L, et al. The effect of *Helicobacter pylori* treatment on remission of idiopathic central serous chorioretinopathy. Mol Vis. 2011; 17:99–103. serial online. Available at: http://www.molvis.org/molvis/v17/a13/. [PubMed: 21245962]
22. Imamura Y, Fujiwara T, Margolis R, Spaide RF. Enhanced depth imaging optical coherence tomography of the choroid in central serous chorioretinopathy. Retina. 2009; 29:1469–73. [PubMed: 19898183]
23. Kim YT, Kang SW, Bai KH. Choroidal thickness in both eyes of patients with unilateral active central serous chorioretinopathy. Eye (Lond). 2011; 25:1635–40. [PubMed: 22020172]
24. Drexler W, Fujimoto JG. State-of-the-art retinal optical coherence tomography. Prog Retin Eye Res. 2008; 27:45–88. [PubMed: 18036865]
25. Regatieri CV, Branchini L, Fujimoto JG, Duker JS. Choroidal imaging using spectral-domain optical coherence tomography. Retina. 2012; 32:865–76. [PubMed: 22487582]
26. Spaide RF, Koizumi H, Pozzoni MC. Enhanced depth imaging spectra-domain optical coherence tomography. Am J Ophthalmol. 2008; 146:496–500. [PubMed: 18639219]
27. Potsaid B, Baumann B, Huang D, et al. Ultrahigh speed 1050nm swept source/Fourier domain OCT retinal and anterior segment imaging at 100,000 to 400,000 axial scans per second. Opt Express. 2010; 18:20029–48. serial online. Available at: http://www.opticsinfobase.org/oe/abstract.cfm?uri=oe-18-19-20029. [PubMed: 20940894]
28. Motaghiannezam R, Schwartz DM, Fraser SE. In vivo human choroidal vascular pattern visualization using high-speed swept-source optical coherence tomography at 1060 nm. Invest Ophthalmol Vis Sci. 2012; 53:2337–48. [PubMed: 22410568]
29. Unterhuber A, Považay B, Hermann B, et al. In vivo retinal optical coherence tomography at 1040 nm - enhanced penetration into the choroid. Opt Express. 2005; 13:3252–8. serial online. Available at: http://www.opticsinfobase.org/oe/abstract.cfm?uri=oe-13-9-3252. [PubMed: 19495226]
30. American National Standard for Safe Use of Lasers. Laser Institute of America; Orlando, FL: 2007. ANSI Z136.1-2007. Available at: http://www.lia.org/PDF/Z136_1_s.pdf [Accessed September 29, 2013]
31. Kraus MF, Potsaid B, Mayer MA, et al. Motion correction in optical coherence tomography volumes on a per A-scan basis using orthogonal scan patterns. Biomed Opt Express. 2012; 3:1182–99. serial online. Available at: http://www.opticsinfobase.org/boe/fulltext.cfm?uri=boe-3-6-1182&id=233031. [PubMed: 22741067]
32. Gorczynska I, Srinivasan VJ, Vuong LN, et al. Projection OCT fundus imaging for visualizing outer retinal pathology in non-exudative age related macular degeneration. Br J Ophthalmol. 2009; 93:603–9. [PubMed: 18662918]

33. Margolis R, Spaide RF. A pilot study of enhanced depth imaging optical coherence tomography of the choroid in normal eyes. Am J Ophthalmol. 2009; 147:811–5. [PubMed: 19232559]
34. Spaide R. Autofluorescence from the outer retina and subretinal space: hypothesis and review. Retina. 2008; 28:5–35. [PubMed: 18185134]
35. van Velthoven ME, Verbraak FD, Garcia PM, et al. Evaluation of central serous retinopathy with en face optical coherence tomography. Br J Ophthalmol. 2005; 89:1483–8. [PubMed: 16234458]
36. Prunte C, Flammer J. Choroidal capillary and venous congestion in central serous chorioretinopathy. Am J Ophthalmol. 1996; 121:26–34. [PubMed: 8554078]
37. Tewari HK, Gadia R, Kumar D, et al. Sympathetic-parasympathetic activity and reactivity in central serous chorioretinopathy: a case-control study. Invest Ophthalmol Vis Sci. 2006; 47:3474–8. [PubMed: 16877418]
38. Piccolino FC, Borgia L. Central serous chorioretinopathy and indocyanine green angiography. Retina. 1994; 14:231–42. [PubMed: 7973118]
39. Tittl MK, Spaide RF, Wong D, et al. Systemic findings associated with central serous chorioretinopathy. Am J Ophthalmol. 1999; 128:63–8. [PubMed: 10482095]
40. Haimovici R, Koh S, Gagnon DR, et al. Risk factors for central serous chorioretinopathy: a case-control study. Ophthalmology. 2004; 111:244–9. [PubMed: 15019370]
41. Guyer DR, Yannuzzi LA, Slakter JS, et al. Digital indocyanine green videoangiography of central serous chorioretinopathy. Arch Ophthalmol. 1994; 112:1057–62. [PubMed: 8053819]
42. Inoue R, Sawa M, Tsujikawa M, Gomi F. Association between the efficacy of photodynamic therapy and indocyanine green angiography findings for central serous chorioretinopathy. Am J Ophthalmol. 2010; 149:441–6. [PubMed: 20172070]
43. Rouvas A, Stavrakas P, Theodossiadis PG, et al. Long-term results of half-fluence photodynamic therapy for chronic central serous chorioretinopathy. Eur J Ophthalmol. 2012; 22:417–22. [PubMed: 21928269]

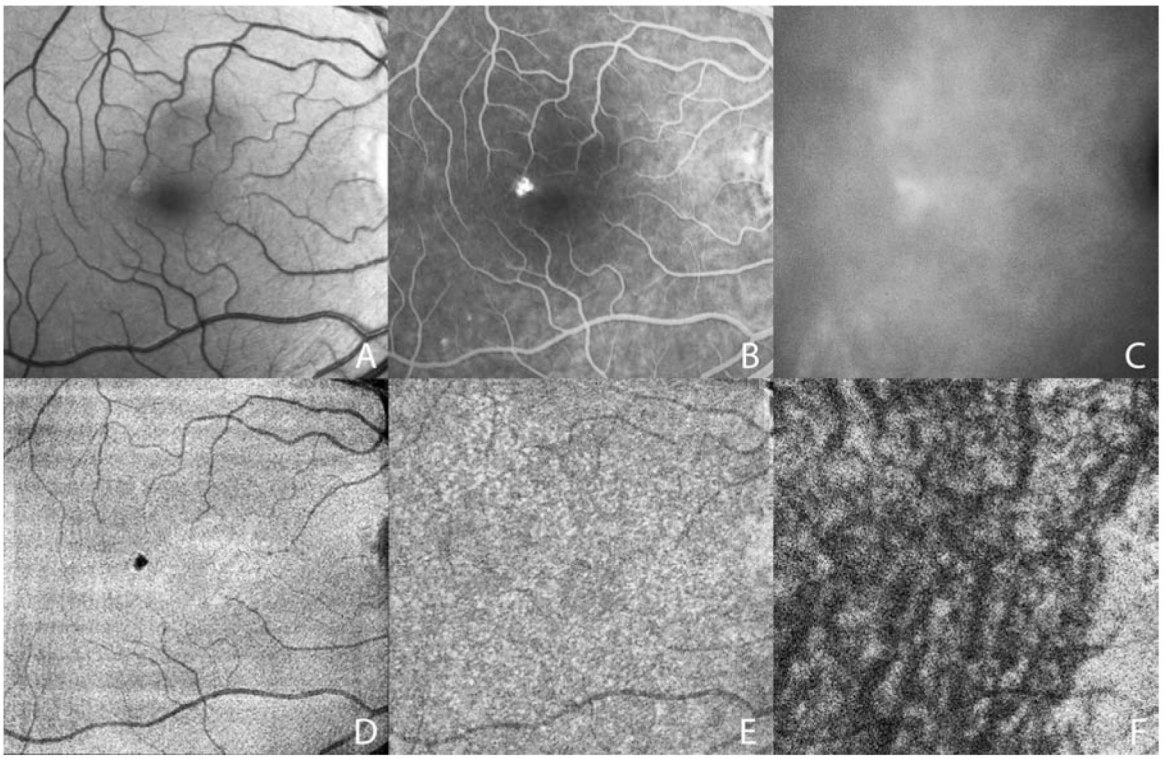

Figure 1.

Patient with chronic central serous chorioretinopathy in both eyes and a small pigment epithelium detachment (PED) close to the fovea in the right eye. Red-free image (**A**) and fluorescein angiography (**B**) show a focal change in the retinal pigment epithelium (RPE), while indocyanine-green angiography (**C**) shows an area of focal hyperfluorescence in the topography of the PED, and widespread hyperfluorescence suggesting increased choroidal permeability. En face swept-source optical coherence tomography (SS-OCT) image at the level of the RPE layer (**D**) reveals a small, focal hyporeflective area correspondent to the PED. En face SS-OCT imaging at the level of the choriocapillaris 40 μm bellow the RPE (**E**) is unremarkable; and at the level of large choroidal vessels 190 μm bellow the RPE (**F**) reveals diffuse choroidal dilation. The white area in the en face OCT image (**F**) shows the choroidal-scleral interface.

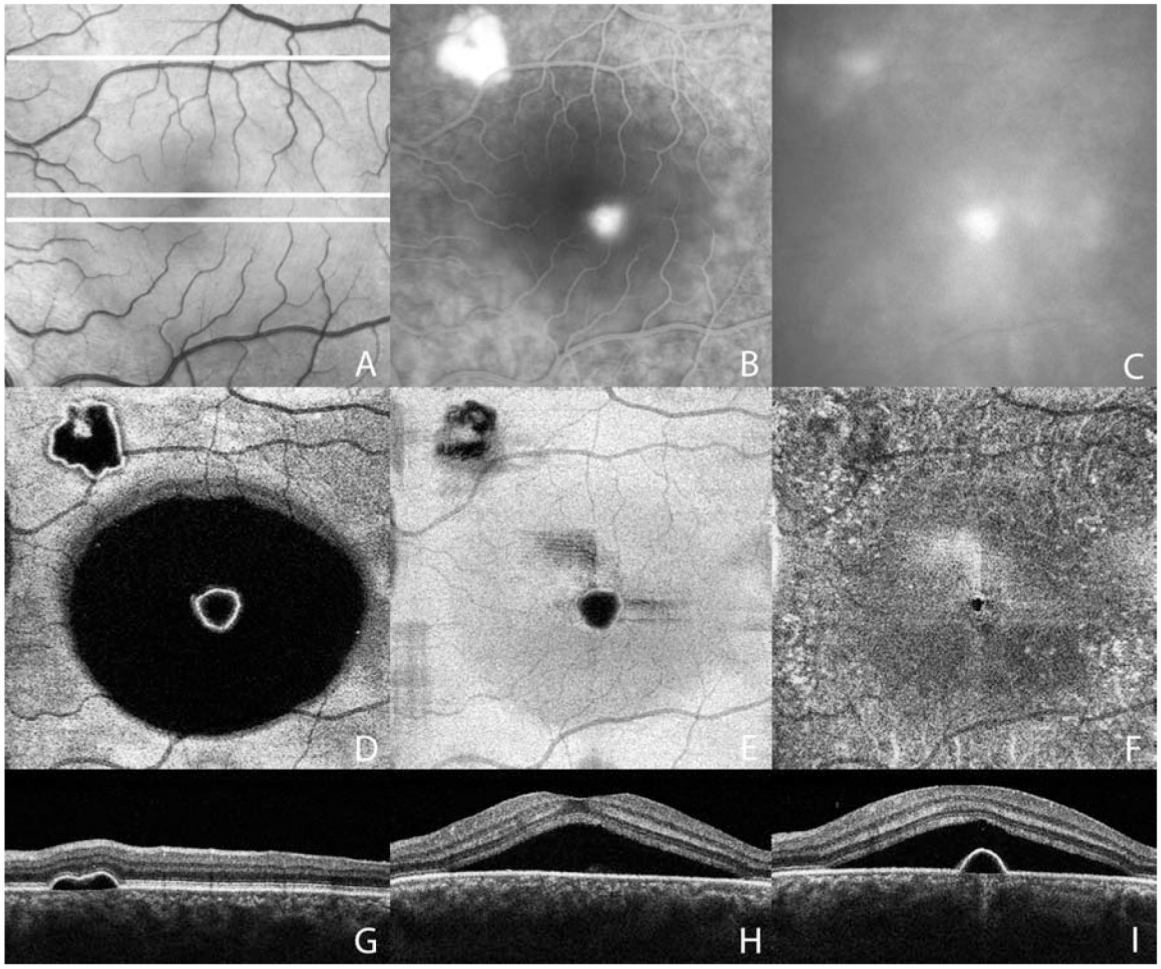

Figure 2.

Patient with chronic central serous chorioretinopathy and serous neurosensory retinal detachment evident on red-free fundus image (**A**). Fluorescein angiography (**B**) reveals two hyperfluorescent areas; the superior one corresponding to a pigment epithelium detachment (PED) and the inferior one corresponding to dye leakage in the “ink dot sign” typical of the disease. Late-phase indocyanine-green angiography (**C**) shows a hyperfluorescent spot in this same topography, surrounded by multifocal choroidal hyperfluorescence. En face swept-source optical coherence tomography (SS-OCT) image 30 μm above the retinal pigment epithelium (RPE) level (**D**) with dark areas corresponding to subretinal or sub-RPE fluid; the large area with “smooth” borders corresponds to the serous neurosensory retinal detachment, while the two small areas with a distinct white hale corresponds to PEDs. En face SS-OCT image at the RPE level (**E**) revealing RPE defects at the topography of the PEDs; and 30 μm bellow the RPE level (**F**) with a focal dilation in the choriocapillaris at the same topography of the central lesion. Cross-sectional b-scans from the areas indicated in A, respectively, showing the PED superior to the fovea (**G**); the serous neurosensory retinal detachment involving the fovea (**H**); and the central PED within the retinal detachment (**I**).

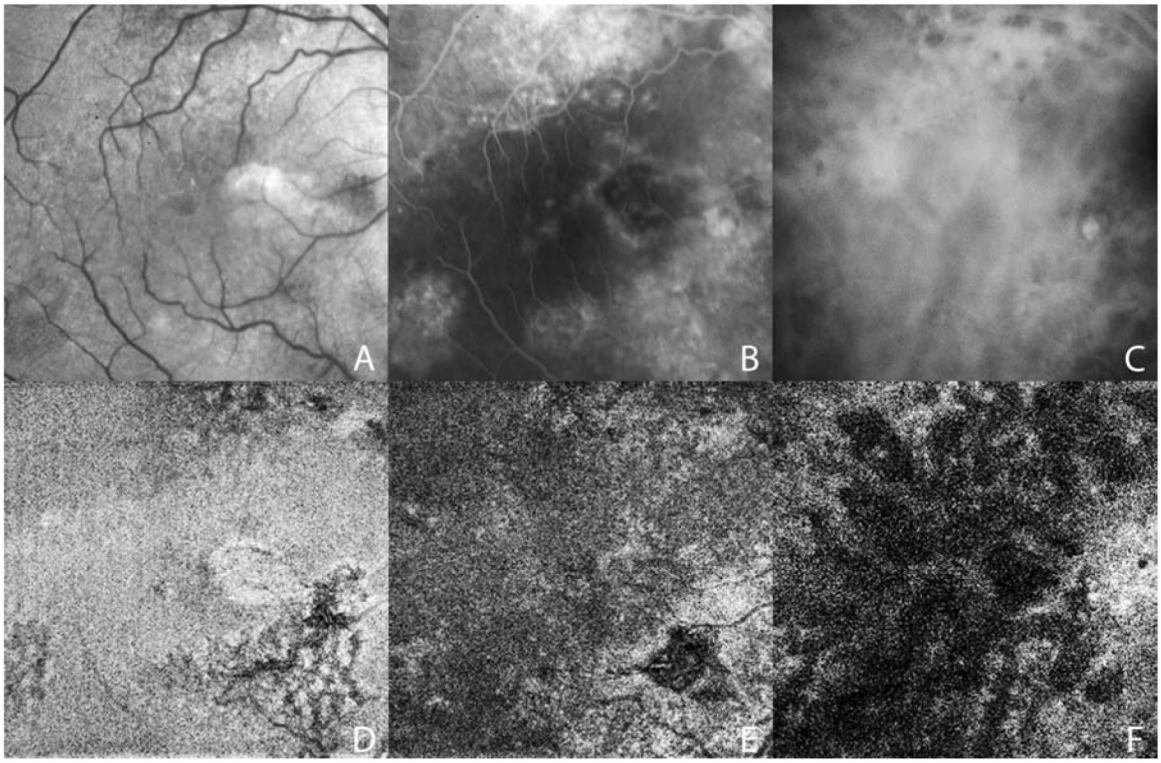

Figure 5.
Patient with chronic central serous chorioretinopathy and subretinal fibrosis due to secondary choroidal neovascularization (CNV), evident on red-free fundus image (**A**). Fluorescein angiography (**B**) documents widespread retinal pigment epithelium (RPE) changes around the fibrosis, which blocks the background fluorescence. Middle-phase indocyanine-green angiography (**C**) suggests a polypoidal-like neovascular lesion. En face swept-source optical coherence tomography (SS-OCT) image at the level of the RPE (**D**) reveals the neovascular network extending from the fibrosis. En face SS-OCT image 25 μm bellow the RPE (**E**) reveal distinct focal choroidal dilation at the level of the choriocapillaris; while diffuse choroidal dilation was observed on medium and large vessels layers as seen on a en face OCT image at 250 μm bellow the RPE level (**F**).

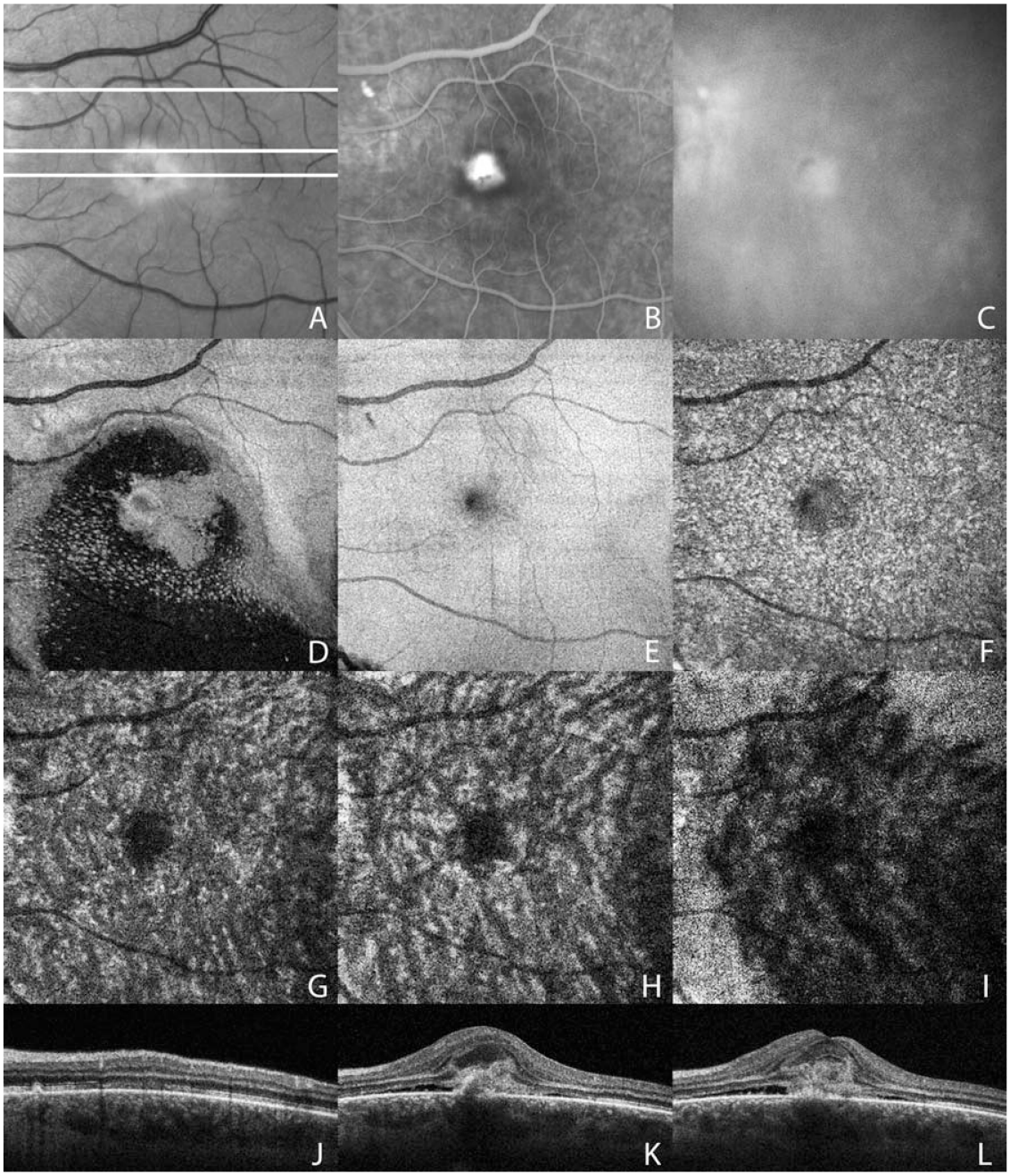

Figure 6.

Patient with chronic central serous chorioretinopathy and subfoveal secondary choroidal neovascularization (CNV) evident on red-free fundus image (**A**). Fluorescein angiography (**B**) shows the hyperfluorescent active CNV, which appears as a hyperfluorescent spot in the late-phase indocyanine-green angiography (**C**). En face swept-source optical coherence tomography (SS-OCT) image 30 μm above the RPE (**D**) delineates the area of subretinal fluid, appearing in dark. En face SS-OCT image at the level of the retinal pigment epithelium (RPE)(**E**) shows a focal RPE loss in the center of the neovascular complex, appearing in dark, and an additional dark spot corresponding to a small pigment epithelium

detachment (PED). En face SS-OCT image 40 μm bellow the RPE (**F**) reveals distinct area of focal choroidal dilation that extends from the choriocapillaris throughout the choroid, also evident on en face images at 120 μm (**G**), 160 μm (**H**), and 260 μm (**I**) bellow the RPE. Note in I that this distinct area of focal choroidal dilation seems to have anatomical connection to a large, dilated choroidal vessel. Cross-sectional b-scans from the areas indicated in A, respectively, the small PED (**J**); and the point of RPE rupture confirmed by the en face image on E (**K**). The focal choroidal dilation clearly documented on en face images is not visible on the b-scan through the fovea (**L**).